Lab on a Chip

Accepted Manuscript

ROYAL SOCIETY OF CHEMISTRY

www.rsc.org/loc

Microfluidic spinning of micro- and nano-scale fibers for tissue engineering

Yesl Jun[1], Edward Kang[2,3], Sukyoung Chae[4], Sang-Hoon Lee[1,2]*

[1]Biotechnology-Medical Science, KU-KIST Graduate School of Converging Science and Technology, Korea University, Seoul 136-701, Republic of Korea

[2]Department of Biomedical Engineering, College of Health Science, Korea University, Seoul 136-703, Republic of Korea.

[3]Department of Medicine, School of Medicine, Korea University, Seoul 136-713, Republic of Korea.

[4]Harvard-MIT Division of Health Sciences and Technology, Massachusetts Institute of Technology, Cambridge, Massachusetts 02139, USA

***Corresponding author:**

Sang Hoon Lee, Ph.D.

Professor

Department of Biomedical Engineering,

College of Health Science, Korea University

Jeongneung 3-dong, Seongbuk-gu,

Seoul 136-703, Republic of Korea

Tel: +82 2 940 2881, Fax: +82 2 921 6818

E-mail: dbiomed@korea.ac.kr

Abstract

Microfluidic technologies have recently been shown to hold significant potential as novel tools for producing micro- and nano-scale structures for a variety of applications in tissue engineering and cell biology. Over the last decade, microfluidic spinning has emerged as an advanced method for fabricating fibers with diverse shapes and sizes without the use of complicated devices or facilities. In this critical review, we describe the current development of microfluidic-based spinning techniques for producing micro- and nano-scale fibers based on different solidification methods, platforms, geometries, or biomaterials. We also highlight the emerging applications of fibers as bottom-up scaffolds such as cell encapsulation or guidance for use in tissue engineering research and clinical practice.

1. Introduction

Tissue engineering is one of hottest emerging topics in the biomedical engineering field and has played a key role in extending therapeutic approaches toward the replacement and regeneration of organs. The field of tissue engineering combines engineering (mainly material and mechanical engineering) with the life sciences in an effort to develop diverse biological substitutes that can restore, maintain, or improve organ function.[1] Tissue engineering or organ regeneration applications require the following essential technical features: i) large numbers of cells with a specific lineage, ii) a scaffold that provides an architecture on which seeded cells can organize and develop into a desired organ or tissue prior to implantation, iii) the provision of suitable biochemical and physiochemical factors for enhancing the functions of the biological substitute, and iv) the engineered tissues must be immunoprotective.[2] Recent splendid progress in stem cell research, including study on embryonic stem cells (ESCs) and induced pluripotent stem cells (iPSCs), has enabled the generation of large numbers of multipotent stem/progenitor cells as sources of lineage-committed mature cells that can be used to create tissue constructs. The organization of excellent biomimetic platforms that can bridge between the biological and engineering requirements, as observed in the *in vivo* microenvironment, remains a challenge.[3-5] Such platforms play a pivotal role in the construction of well-defined tissues. The modalities of these platforms in *in vitro* and *in vivo* environments and the ability of the materials to provide a supporting matrix scaffold upon which cells and tissues can grow are important features of good biomimetic platforms.

Scaffolds are porous biodegradable structures fabricated from either synthetic polymers or natural materials and are key to supporting proliferation, differentiation, cell-cell signaling, biomolecule production, and the formation of extracellular matrices in tissue engineering.[6] Most scaffolds are manufactured into highly porous sponge-like sheets, foams, highly complex structures, or matrices and can be designed to influence the chemical, mechanical, physical, and biological environment surrounding a cell population. The basic requirements of a good scaffold are[7]: (i) suitable macrostructure to promote cell proliferation, (ii) well-defined pore geometry with a highly porous surface and microstructure that enables cell growth, (iii) optimal pore size for encouraging tissue regeneration and avoiding pore occlusion, (iv) suitable surface morphology and physiochemical properties for encouraging intracellular signaling, cell recruitment, and guided cell growth. In addition, a scaffold material must degrade at a predictable rate and display clinical-grade biocompatibility. In an effort to fabricate scaffolds using suitable materials, a variety of methods have been developed, including solvent casting,[8, 9] freeze drying,[10, 11] phase separation,[12-14] and gas foaming.[15] Although the pore size, porosity, and interconnectivity may be comparatively well-controlled using these methods, fine control over the shape, spatio-temporal positioning of the chemical composition, and alignment for aligned cell culture and microscale extracellular matrix (ECM) still pose significant challenges. Recent progress in the silicon and electromechanical technologies of microstereolithography[16] and rapid prototyping[17, 18] has enabled the production of finely-defined scaffolds; however, the costs associated with these techniques are high, and well-trained skillful labor is required. Technologies that could enable the facile spatio-temporal positioning of chemical compositions require further development. Fabrication of scaffold networks composed of micro- and nano-fibers is emerging technology to address many problems of scaffolds previously mentioned. In the human body, connective tissues are formed by a network of cells and fibrous extracellular matrices.[19] Fibers, including collagen, play an important role in maintaining tissue structure; in fact, type-I collagen makes up about 25% of the total protein content of a mammalian body.[20] Fibrous scaffolds have attracted attention for their utility as

scaffolds that can guide cell growth, cell networking, and enable fine control over the scaffold porosity. Recent progress in electro-spinning technologies has led to the development of nanofiber-based ECMs with a diversity of shapes and sizes that can be broadly used as biomimetic scaffolds because they provide networked structures similar to collagen.[21] Electrospun scaffolds are advantageous because their fiber diameters are comparable to those found in the native extracellular matrix and the electrospinning technique can align the fibers within the scaffold to control and direct cellular interactions and matrix deposition.[22] Due to the high surface area-to-volume ratio of electrospun fibers, a high voltage (from 5 to 50 kV) must be applied to successfully pull the charged solution. Such high voltages unfortunately preclude the loading of sensitive biological materials into the solution. Beads can occasionally form in the fiber structure due to the presence of unstable polymer solution jets with a high surface tension. The construction of a large 3D scaffold volume in which the molecular configurations, orientations within the fiber structure, and cell encapsulation may be controlled such that the matrix is non-immunogenic faces several challenges before clinical applications may be realized. Alternative microfluidic spinning approaches have been developed to address these limitations.

Microfluidic technologies have recently shown significant potential as novel tools for producing micro- and nano-scale structures with a diversity of shapes, including particles, fibers, and tubes, without the use of complicated devices or facilities, and the produced structures can be used as bottom-up scaffolds.[23, 24] Structures prepared using controlled patterning and bearing porous morphologies and controlled fiber sizes have been used as scaffolds. Biological materials, including cells, may be readily loaded into fibers prepared using microfluidic technologies. An exciting recent development in the area of microfluidic spinning systems was the demonstration of physicochemically coded fibrous scaffolds based on calcium alginate. Microfluidic spinning technologies are emerging as advanced tools for a variety of applications in tissue engineering and cell biology.

This review presents an overview of diverse microfluidic technologies and their potential applications in tissue engineering, such as the fabrication of micro- and nano-scale scaffolds or cell encapsulation. After a brief description of the system requirements for and principles underlying microfluidic systems, we will categorize the spinning methods into: microfluidic spinning platforms, polymerization methods, and the preparation of diverse fiber shapes, including solid, tubular, flat, and so forth (Fig 1, left). Diverse fibers encapsulating cells and fibers on which cells were culturing in a guided manner are described (Fig 1, right), and their applications in tissue engineering are noted. Future directions of microfluidic spinning will involve exploring the preparation of cell-laden fibers in specific shapes suitable for organ function and implantation into the body.

2. System requirements and principles of microfluidic systems

Fluid flow in microfluidic systems is usually laminar due to the channel size.[25] Two or more streams flowing in contact with one another, therefore, will not mix except by diffusion at the interface.[26] Phase separation in microfluidic channels enables the formation of coaxial flow, and fibers can be produced by solidifying the central flow using photopolymerization and ion crosslinking processes, as shown in Fig. 2. A polymerizable sample fluid and non-polymerizable sheath fluid are introduced into separate input ports and meet at a channel intersection. Through microscale effects, the 3-D coaxial sheath flow stream surrounds the sample flow. The radius of the sample stream within the sheath flow can be modulated without retooling, and can be described as a function of the volume flow rates of the sample and sheath streams.[27, 28] In a cylindrical channel, the diameter of the central flow, R_s, may be described as a function of the sample stream and total

volume flow rate.[27]

$$R_s = R\left[1 - \left(\frac{Q_{sheath}}{Q_{sample} + Q_{sheath}}\right)^{1/2}\right]^{1/2}$$

where R is the channel radius. The total volume flow rate, Q, is given by the sum of the sample volume flow rate, Q_{sample}, and the sheath volume flow rate, Q_{sheath}.

During fiber formation using microfluidic techniques, the moving central flow should solidify as fast as possible, for example, using polymer chain crosslinking by photopolymerization, or chemical reactions. Photopolymerization may be accomplished by mixing the UV-polymerizable backbone material with a photoinitiator prior to injection (Fig. 2(a)). A prepolymer may be introduced into the microfluidic channel, and scaling effects induce the formation of a coaxial flow shape from a separated central flow (prepolymer) and sheath flow. Poly(ethylene glycol) diacrylate (PEG-DA)[29-34] or 4-hydroxybutyl acrylate (4-HBA)[34-36] are generally used as a backbone material because the polymerization time is fast. UV light (365 nm) is then directed onto the flow stream to initiate photopolymerization as the coaxial flow travels through the microchannel. The solidified fibers are then extruded out. The sheath flow acts as a lubricant to facilitate fiber extrusion, and its viscosity must be similar to that of the central flow. PVA is generally a good sheath fluid material because its viscosity may be readily controlled and it is not harmful. The main advantages to the photo-polymerization method are that the polymerization process is simple and stable. Photopolymerization is limited, however, in that UV radiation may be harmful to sensitive bioactive species, and the material is not biodegradable. For this reason, photopolymerized fibers are not suitable for scaffold applications.

Fast chemical reactions between the central and sheath fluids may be used to prepare diverse microfibers from different materials (Fig. 2(b)). The most popular central fluid materials for ECM or biomedical applications are alginate,[37-55] PLGA,[56-58] and chitosan.[59-61] For the microfluidic spinning of alginate fibers, a sodium alginate solution is introduced into a sample channel and a $CaCl_2$ solution is introduced into a sheath channel. At the interface between the two fluids, sodium alginate is cross-linked due to the diffusion of Ca^{2+} ions into the alginate solution. The solidified alginate fibers are then extruded through an outlet channel. PLGA microfibers have been developed using PLGA and glycerin solutions in place of alginate and $CaCl_2$, respectively. Although chemical polymerization methods have their limitations and difficulties associated with shape formation, they are very useful for biomedical production applications because most of the materials used in chemical polymerization reactions are biocompatible and biodegradable. Successful chemical spinning approaches rely on the use of a suitable central and shear fluid pair. Recently, diverse biomedically applicable materials have been used as fiber materials. Table 1 summarizes the solidification methods and materials that have been tested for use in microfluidic spinning.

3. Platforms for fiber generation

Cylindrical channels facilitate control over the flow parameters during coaxial flow creation. For this reason, devices used for fiber generation have been developed using pulled glass micropipettes, cylindrical or rectangular PDMS microchannels, metal needles, or tubes (Fig. 3). Glass has several advantages as a material for microfiber fabrication: (i) the glass surface is hydrophilic, (ii) the cross-section of a glass capillary tube is perfectly cylindrical in shape, so that a polymerizable sample can form a stable co-axial flow, and (iv) the glass

surface may be readily modified to allow the use of diverse materials for fiber generation. We developed a microfluidic fiber spinning chip consisting of pulled and regular glass capillaries integrated using a PDMS support channel.[34, 36, 39, 45, 46, 49, 53, 54, 56, 57, 60, 61] Two concentric capillaries, pulled and regular, may be inserted into pre-perforated PDMS base holes. The Takeuchi group spun a hollow microfiber using a double coaxial laminar flow microfluidic device composed of two pulled and one regular glass capillary, integrated using two plastic-based connectors.[44, 62, 63] Although capillary-based platforms are low-cost and advantageous for creating coaxial flows, the preparation of pulled glass micropipettes is labor-intensive and requires a high level of skill. Several capillary-free PDMS spinning chips have been developed such that the cross-sectional shape of the spinning channel produces diverse fibers. Choi et al. fabricated complex-shaped microfibers, such as single- and double-hollow microfibers and micro belts, using the spontaneous formation of a jet stream.[32] Unlike other microfluidic approaches to the formation fibers, they used a microfluidic platform with a rectangular channel and relied on the minimization of the interfacial free energy to form a circular fiber cross-section. Two dispersed fluids were injected, the polymerizing fluid and the liquid template stream, and floating central streams formed a cylindrical shape within an outer immiscible fluid. The Shoji group developed a slightly more complicated microfluidic channel that could autonomously induce coaxial flow through the structure of channel's inner geometry.[64, 65]

Kang et al. recently developed a PDMS microfluidic chip having cylindrical channels and valves that could replace micropipette-based spinning chips.[48] This microfluidic chip could be combined with a digital fluidic controller and valve to successfully code diverse chemical compositions, structures, gas bubbles, live cells, and morphologies into and onto the microfibers. These systems have broken several barriers to conventional fiber generation platforms, including: (1) the preparation of fibers with complex morphologies and tunable compositions; (2) the development of low-cost facile devices that can replace glass capillaries; and (3) the combination of various microfluidic chip designs for fiber generation. Non-cylindrical microfiber shapes have been prepared using PDMS microfluidic chips, including flat fibers, grooved fibers, and belts, through the use of devices having rectangular channels.[33, 48, 50, 52] Depending on the shape of the channel cross-section, a variety of patterns may be engraved onto the surfaces of the fibers along the longitudinal direction. Thin and flat channels may be used as platforms for continuously spinning flat fibers. Longitudinal grooves on the inner surfaces of cylindrical channels can enable the spinning of microfibers bearing grooved surfaces.

4. Microfluidically spun fibers with diverse shapes and dimensions

The aforementioned microfluidic spinning platform has been used to produce diverse fiber shapes. Table 2 summarizes the shapes of the fibers according to the spinning method and materials. The diverse shapes prepared using microfluidic spinning techniques are summarized in the following discussion.

4.1. Solid fibers

The most popular microfluidic-spun fiber shape is the solid cylindrical shape. These fibers are comparatively easy to spin and can readily encapsulate cells without seriously damaging the cells. Such solid fibers have been produced by both photo and chemical reactions. Jeong et al. reported the first successful spinning of fibers using microfluidic approaches.[34] 4-HBA was used as the backbone material, and 364 nm UV light was used for the photopolymerization reaction. They also reported the preparation of tubular or Janus fibers consisting of 2 different materials with potential utility in pH-responsive fabrics. Although 4-HBA is an

attractive material, it is limited in its applicability toward the biomedical areas because it is not biodegradable and its biocompatibility has not been established. PEG-DA is an excellent biocompatible and photo-curable material for use in microfluidic spinning applications; however, its poor biodegradability has hindered its utility in applications. Shin et al. demonstrated the spinning of solid and cylindrical alginate fibers, which are known to have excellent biocompatibility and biodegradability, using fast chemical reactions between sodium alginate and $CaCl_2$ solutions.[45] The reaction between sodium alginate and $CaCl_2$ is usually slow, but the fiber polymerization reaction occurred very fast on the microfluidic device (< a few hundred milliseconds) due to the microscale distances over which diffusion was required. Decreasing the flow diameter to the hundred-micron scale resulted in the rapid polymerization of the liquid sodium alginate in the presence of Ca^{2+} ions during passage through the outlet channel. Cells could be readily encapsulated in the alginate fibers. For example, fibroblast-encapsulated alginate fibers were prepared and the cells were shown to be alive after encapsulation for 1 day. Several solid and cylindrical alginate fibers were fabricated using a microfluidic spinning platform, and researchers demonstrated the potential of these fibers in tissue engineering applications.[44, 48, 66, 67] Diverse cells, including NIH-3T3/HeLa, rat hepatocyte, fibroblast, and rat islet cells, have been encapsulated in fibers, with successful maintenance of the cell viability and function. Microfluidic spinning methods appear to be safe for cell encapsulation applications, unlike electro-spinning or melt-spinning techniques. An array of alginate hydrogel microfibers can be produced with the specially designed microfluidic tools. Raof et al. fabricated long microfibers and microtubes through the use of a microfabricated SU-8 filter device by means of capillary action, and they demonstrated the encapsulation of mouse ES cells.[68] Their approach is advantageous for producing large quantities of cell-encapsulated fibers. Several materials other than alginate have been used to fabricate solid ECM threads, including chitosan, PLGA, and amphiphilic ABA triblock copolymers.[69] Lee et al. prepared microfluidic-spun solid chitosan fibers and used them to culture HepG2 cells to realize the liver on a chip.[60] The cells grew in clusters around the chitosan fibers and secreted albumin and urea, which are basic requirements of liver function. Hwang et al. spun PLGA fibers and seeded fibroblasts on the surfaces of these fibers (Fig. 4a).[56, 57] Interestingly, the shape of cells was changed to the diameter of fibers and the cells were aligned well along the longitudinal direction of the fibers with diameters less than 20 microns.

4.2. Tubular fibers

Tubular fibers have several advantages in tissue engineering applications. Onoe et al. reported the use of tubular fibers for the engineering of long thread-based tissues.[44] They spun tubular alginate fibers into which cells and ECM proteins had been encapsulated. The encapsulated cells were cultured in the fibers and, finally, the encapsulating alginate dissolved away. A thin (approximately 100 μm), long (greater than a meter), and easily manipulated cellular construct, termed a cell fiber, was created through this process, which preservation of the intrinsic cellular morphologies and functions. The tubular fibrous structure allowed cells to migrate and connect to on another three-dimensionally. This method can enable the engineering of long thin neurons or muscle cell fibers that are not accessible using conventional tissue engineering methods. Vascularization is another critical application of tubular fibers. Lee et al. reported the synthesis of cell-laden and protein-immobilized hollow alginate fibers and the in situ alignment of the fibers.[46] The endothelial cell-laden tubes supported cell viability, indicating that the mild fabrication process was biocompatible. Vascular tissue was emulated by embedding endothelial cells in the hollow fibers to form smooth muscle cell-laden agar–gelatin–

fibronectin (AGF) hydrogels. Cells within the hollow fibers and hydrogels were co-cultured and remained alive with an intact vascular structure for 7 days. Hu et al. spun hollow fibers using diverse materials, such as Gtn-HPA hydrogels, poly-(N-isopropyl acrylamide) (poly(NIPAAM)), and polysulfone.[70] They immobilized live cells and biological components (e.g., growth factors, ECM, drugs, proteins, and nutrients) within the hydrogel matrix. Choi et al. fabricated various complex-shaped microfibers, including single- and double-hollow microfibers, based on the concept of minimizing the interfacial free energy (Fig. 4b).[32] Asthana et al. trapped a marine metalloenzyme, the vanadium-containing bromoperoxidase (VBPO) enzyme isolated from *Corallina confusa*, in a hollow alginate microfiber and used this fiber as a microfluidic bioreactor to demonstrate the bromo-oxidation of Phenol Red to Bromophenol Blue.[49] They demonstrated the use of hollow fibers as tubular biosensors. Similar arrayed methods for simultaneously spinning solid fibers, such as tubular alginate microfibers, have been demonstrated using arrays of micro-hole. Oh et al. developed a microfluidic method for generating cell-adhesive chitosan microtubes in a single fabrication step using a glass capillary system. This approach involved the potential use of diverse hydrogels.[61] Hollow fibers may be broadly used in biomedical areas, including hemodialysis filters and bio-artificial livers; however, downsizing the sizes of fibers and controlling the fiber porosity pose significant challenges, and we expect that this microfluidic spinning technology may break the limitations imposed by conventional methods.

4.3. Hybrid (Janus) fibers

Microfluidic spinning methods enable the production of Janus fibers, in which heterogeneous materials and cells may be readily spatio-temporally positioned. Jeong et al. reported the preparation of photopolymerized Janus fibers by simultaneously injecting two different solutions (colored and non-colored 4-HBA).[34] Jung et al. spun asymmetrically structured (Janus) microfibers using a microfluidic device and the aqueous photopolymerization reaction of photocurable polyurethane (PU) (NOA63; Norland Optical Adhesive) (Fig. 4c, top).[71] The aqueous solution was injected into the microfluidic chip, and UV light was directed over the flow. During the spinning process, bubbles of carbon dioxide formed upon the reaction of the isocyanate groups of NOA with the water molecules absorbed from the aqueous continuous phase. The bubbles migrated toward the upper surface of the polymerizing PU fiber, where asymmetric porous structures formed spontaneously. Recently, Kang et al. proposed a novel spinning method that used a microfluidic chip combined with a digital fluid controller (Fig. 4c, bottom).[48] Active functional modulations were introduced, for example, by switching the flow using a digital controller scheme. They produced microfibers with spatiotemporal coding of diverse chemical compositions, structures, gas bubbles, live cells, and morphologies. They also fabricated coaxial fibers for the co-culturing of heterogeneous cells. They spun fibers configured such that rat hepatocytes and fibroblasts were localized at the fiber center and a peripheral coaxial layer of cells encapsulated the fiber. The encapsulated cells were then co-cultured. The experimental results showed that co-culturing enhanced the viability of both cells compared with the hepatocyte mono-cultured configuration. A few microscale grooves could be engraved on the surfaces of the microfibers having diameters of a few tenth of a micron simply by changing the structure of the channel's inner surface. Neuron cells were cultured on the grooved surfaces to form an aligned neural network. In living creatures, the spatio-temporal positioning of different materials and structures at the nano- and micro-scale facilitates the growth of organs or structures. Methods for spinning hybrid fibers could enable the development of super materials, such as spider silk or sea shells.[72-75]

4.4. Flat fibers

Unlike conventional spinning methods, microfluidic spinning methods can be used to fabricate flat fibers, and several types of information can be encoded using specially designed microfluidic chips or computer-controlled switching. Kim et al. described the first demonstration of the continuous microfluidic spinning of polymeric barcoded microstrips using a flat channel. These microstrips were used to demonstrate utility in multiple biocatalyst-based sensing systems (Fig. 4d, top).[33] As an interesting application, they fabricated a pH-responsive actuation component in which the actuation region could be programmed by coding different materials into the strip. Leng et al. fabricated hydrogel sheets with millimeter to centimeter length scales in an effort to form 2D or 3D soft material assemblies.[52] Within the unsuspended hydrogel sheets, diverse information could be stored, including void regions, to create a mosaic stiffness with diffusivity patterns. The sheet could be tessellated with different viable primary cells (rat cardiomyocytes, etc.) to prepare a useful 3D tissue organization structure. The proposed mosaic tessellating method permitted spatiotemporal control over the hydrogel composition, allowing for the encoding of information in the soft material at a resolution of approximately 130 μm with a 50 ms response time. Cho et al. described the preparation of a microfluidic spinning platform for the formation of stratified laminar flows that could generate rectangular hydrogel microfibers with a variety of compositions.[30] They employed double-layer microfluidic devices to produce a photopolymerizable core liquid flow with two inert carrier liquid flows for the continuous fabrication of microfibers. The dimensions and chemical compositions of the microfibers could be readily manipulated by controlling the flow rates and compositions of the core liquid flows. Kang et al. proposed the continuous fabrication of flat alginate microfibers (microribbons) with size-tunable grooved microstructures using a microfluidic system (Fig. 4d, bottom).[50] They controlled the number and dimensions of a few micrometer-scale grooves by changing the grooved patterns on the slit-shaped channels.

4.5. Scale-down and crystal-like structures

In principle, the scaling down of structures to the nanometer size using microfluidic spinning platforms is challenging due to the difficulties associated with fabricating nanoscale microfluidic chips and injecting fluids into the narrow channels. Furthermore, the formation of crystalline structures, such as *B. mori* silk during spinning, remains challenging. Chae et al. developed a novel spinning method for creating ultrathin (< 100 nm) and crystal-likely ordered multiple polymeric alginate fibers using a single microfluidic platform (Fig. 4e).[51] The flow was focused to the nanoscale by employing the principle that ionic polymers in low-polarity solvents tend to aggregate due to the attractive forces of the ionic dipoles. Isopropyl alcohol (IPA) was used as a sheath solvent, and the central alginate flow was focused very narrowly to generate an ultra-thin fiber (< 100 nm) using a 100 μm microfluidic channel. The spinning method enabled the self-alignment of polymer chains in the fibers along the direction of flow to form crystal-like ordered structures. They demonstrated that diverse fiber shapes could be prepared simply by controlling the flow rate. Kiriya et al. developed a simple method for fabricating densely aligned supramolecular nanofibers jacketed in a robust hydrogel on the meter length scale using microfluidic techniques.[42] The supramolecules self-aligned under the shear stress provided by the laminar flow in the channel. The alignment of supermolecules or polymer chains may be used to generate new materials that are similar to those found in nature without using complicated or expensive devices and

facilities.

5. Potential applications to tissue engineering, and future directions

Microfluidic spinning methods have several advantages over conventional methods, including flexible applicability across different materials and geometries. Easy modulation of the fiber scale (diameter), from the nanometer scale to a few hundred microns, is a key advantage over existing methods that require some form of retooling to realize different outcomes. Another advantage of the platform is that the fabrication process may be performed under ambient conditions. The fluid is not exposed to high voltages, high temperatures, or high stresses, so that any sensitive biological materials, including cells, may be loaded into the fiber without loss of function. The unique characteristics of microfluidic spinning methods enable the application of fibers to tissue engineering, including the encapsulation of well-organized cells within the fibers and the preparation of structured ECM for cell guidance. Cell encapsulation technologies for immobilizing cells within a semipermeable membrane can protect the cells from both mechanical stress and the host's immune system, allowing for the bidirectional transport of nutrients, oxygen, and wastes.[76] Microfluidic spinning methods offer excellent tools for the fabrication of microfibers that encapsulate cells for tissue and organ engineering applications: the spinning environment is not physically or chemically hazardous to the cells, and cell localization may be regulated autonomously.[77] Onoe et al. recently reported the development of a thin (approximately 100 μm), long (greater than a meter), and manipulatable cell fiber that maintained the intrinsic cellular morphology and function.[44] The creation of cell fibers involved the spinning of a hollow fiber in which were embedded natural ECM proteins and cells. The fiber structure allowed the cells to migrate along the hollow interior and connect to on another autonomously. This group engineered primary cardiomyocyte fibers comprising hollow fibers containing HUVECs for the construction of microvessels, or cortical cell fibers for use as neural systems (Fig. 5a, left). They also fabricated fibers containing primary pancreatic islet cells. Cells were harvested from rats, dissociated, and encapsulated in an interpenetrating network (IPN) hydrogel of alginate and agarose. The 20 cm-long primary islet cell fibers were implanted in diabetic mice, and the blood glucose levels were maintained in the normal range for at least 13 days. Jun et al. fabricated immunoprotective collagen–alginate composite (CAC) fibers including islets harvested from rats and implanted them into the intraperitoneal cavities of streptozotocin-induced diabetic BALB/C mice (Fig. 5a, middle).[67] The blood glucose levels of all diabetic mice returned to normoglycemia within 2–3 days after implantation, and this level was maintained for one month. They also constructed uniform hundred micron-scale cell spheroids consisting of hepatocyte and islet cells harvested from rats, and encapsulated these spheroids within CAC fibers.[66] The fibers were implanted into the intraperitoneal cavities of mice, and the glucose levels of diabetic mice were found to return to normal levels 2–3 days after implantation. These levels were maintained for one month by a small number of islet cells. In general, cell spheroids can mimic the *in vivo* environment to improve cell viability and function. Lee et al. demonstrated the formation of a vascular structure prepared by embedding endothelial cells in the hollow fibers of a 3D hydrogel with smooth muscle cells.[46] Yamada et al. produced complex hepatic micro-organoids composed of primary rat hepatocytes and non-parenchymal cells cultured in anisotropic alginate hydrogel microfibers (Fig. 5a, right).[37] They examined effects of the O_2 tension on the viability and function of the hepatocytes, and they measured the effects of 3T3 cell co-culturing on several hepatic functions. Kang et al. also co-cultured primary hepatocytes (center) from rats and fibroblasts (peripheral) in coaxial microfibers to enhance

cell viability and prepare a liver-mimicking tissue structure.[48] Several cell types, including HepG2, P12, etc., were encapsulated and their functions and viabilities were evaluated for use in the support and regeneration of failed organs.

Cells are generally affected by the morphologies of ECM substrates. Extensive studies of cell guidance using electro-spun nanofibers or micro- and nano-patterned substrates have been reported.[78-80] Significant challenges to applying these patterned cells directly to tissue engineering or organ regeneration applications remain. Microfluidic-spun fibers, by contrast, are free-standing and may be implanted in the body. Such fibers have been used to align myoblast, cardiomyocyte, and neuron cells through guided culturing. Kang et al. engraved microscale grooves on the surfaces of cylindrical alginate fibers (diameter < 100 μm) without using special tools.[48] They then seeded neuron cells onto the grooved fibers (Fig. 5b, left). Interestingly, the neurons were found to align themselves along the grooves. Although the grooved fibers demonstrated an excellent capacity for guiding cell culture, the number of cells that could be seeded on the cylindrical microfibers was small. These limitations were addressed by spinning thin flat microfibers (microribbons) bearing size-tunable grooved microstructures.[50] Guided cell culturing techniques were applied to neuron cells from the embryos of pregnant Sprague Dawley rats on the 16th day of gestation. The cells were seeded on the grooved flat fibers and were found to migrate along the ridges of the grooves to form an aligned neural network. The aligned cells on the grooved flat fibers could be directly implanted in the spines or peripheral nervous system for nerve regeneration. They cultured myoblast cells on the grooved flat fiber cells, and the cells were found to align along the direction of the microgrooves. This finding suggests that the microgrooved flat fibers may be used in regenerative medicine contexts in which the assembly of highly aligned cells is crucial. A significant need exists for the regeneration of tendons, ligaments, blood vessels, and muscle (smooth, skeletal, cardiac). Hwang et al. produced size-controlled (with diameters ranging from 10 to 242 μm) PLGA microfibers to analyze the correlation between the cell alignment and fiber diameter (Fig. 5b, right).[57] Mouse fibroblasts (L929) were cultured on fibers having different diameters. Excellent alignment of the cells was observed for the smaller-diameter fibers.

Future directions for this work will involve research into the formation of 3D cell-encapsulated fiber shapes for the support or regeneration of damaged organs. The manipulation and shape formation of cell-laden alginate fibers is currently made difficult by the mechanical weakness of the fibers and the application of stress to the cells. Problems associated with contamination, fabrication costs, and the labor-intensive nature of fabrication introduce other critical problems. Park et al. developed a microfluidic spinning device for preparing 3D cell-laden fibrous scaffolds using a single microfluidic platform in a one step process without the intervention of an operator.[81] The porosity of the fabricated fibrous scaffold could be regulated, and the encapsulated hepatocytes from rats showed better viability and albumin secretion than cells encapsulated in a bulk hydrogel.

6. Conclusions

Microfluidic systems that enable the continuous extrusion of polymeric microfibers have many advantages: they enable control over the fiber size, they are cost-effective, they simplify the fabrication process, and their flexibility enables the safe loading of biological materials and drugs, including compounds, proteins, enzymes, genes, and cells. The characteristics of a fiber may be controlled and designed according to the solubility, viscosity, surface tension, and diffusion of the feed solutions, which determine the properties of the interface

between fluids in a microchannel. Cell-laden fibers can be implanted into the body and can play a pivotal role in supporting and regenerating failed organs. Fibers can protect encapsulated cells from both mechanical stress and the host's immune system, and they allow excellent bidirectional transport of nutrients, oxygen, and wastes. We expect that microfluidic fiber spinning technologies will contribute significantly to the development and engineering of well-organized 3D tissues.

Acknowledgement

This work was supported by the National Research Foundation of Korea (NRF) grant funded by the Korea government (MEST) (No. 2013046403) and the Converging Research Center Program through the Ministry of Science, ICT and Future Planning, Korea (No. 2013K000377).

Table 1. Solidification methods and materials used in microfluidic spinning applications.

Solidifying method	Material	Cross-linker	Ref.
Photo polymerization	PEGDA	UV (365 nm) light	29-31, 33
	Two hydrophilic oligomeric phases PEGDA		32
	PEGDMA		82
	4-HBA		33-36
	4-HBA/PEGDA		83
	Polyurethane (PU)		71
	Polyurethane acrylate (PUA)		84
	Thiol-ene (PETMP, TATATO)		85
	Mesogen, acrylate		86
Chemical reaction	Alginate	$BaCl_2$	37, 55
		$CaCl_2$	38-50, 52-54
		$CaCl_2$ in IPA	51
	Alginate/polylysine (PLL)	$CaCl_2$	68
	Alginate/collagen	$CaCl_2$, 37°C	44, 62, 63, 66, 67, 87
	Alginate/fibrin	$CaCl_2$, 37°C, thrombin	44
	Alginate/agarose IPN	$CaCl_2$	44
	Alginate/chitosan	$CaCl_2$	39
	Chitosan	Sodium triphosphate	59-61
	Chitosan/gelatin		61
	PLGA	Glycerin	56-58
	Poly(methylmethacrylate) (PMMA) in acetone	Fructose solution	88
	Amphiphilic triblock (PPDO-co-PCL-b-PEG-b- PPDO-co-PCL)	De-ionized water	69
	Gelatin–hydroxyphenylpropionic acid (Gtn–HPA)	HRP/H_2O_2 (enzymatic oxidative reaction, pH4.7)	89
	Gtn-HPA with alginate, poly(NIPAAM) or polysulfone	HRP/ H_2O_2 with $CaCl_2$ or UV light	70
	Vanadium Pentoxide (V2O5)	$CaCl_2$	90
	polyacrylonitrile (PAN), polysulfone (PSF), or polystyrene (PS)	PEG (solvent extraction method)	91
	Polybenzimidazole (PBI)	H_3PO_4/water	92
	Regenerated silk fibroin (RSF)	PEO	73

Table 2. The various fiber shapes produced according to each spinning platform and material, for use in certain tissue engineering applications.

Fiber shape	Spinning platform	Material	Size	Cell approach	Cell type	Remarks	Ref.
Solid	Flexible plastic tube	PUA	A few hundred micron	–	–	Quantum dot-based nanocomposite fiber	84
	Stainless steel tubes (triple-orifice spinneret)	Gtn–HPA	> 20 μm	Encapsulation	Madin–Darby canine kidney (MDCK) cells / NIH-3T3 (mouse embryonic fibroblast) cells	Cell immobilization	89
	Stainless steel syringes (needles)	4-HBA/PEGDA	15-500 μm	–	–	Ceramic/polymer nanocomposite fiber	83
	Coaxial needle set	Alginate	150-200 μm	Encapsulation	Human embryonic kidney (HEK) cells	Encapsulation of fiber in 3D hydrogel for microchannel-like porosity	40
	SU-8 filter	Alginate, alginate/PLL	30-300 μm	Encapsulation	Mouse embryonic stem (ES) cells	Arrayed fiber microstrands	68
	Silicon micro-nozzle array	Alginate	> 120 μm	Encapsulation	Human kidney 293 cells	PLL-coated microtubes	38
	Pulled glass pipettes	Alginate	50 μm	–	–	Encapsulation of supramolecular nanofibers	42
	Pulled glass pipettes in PDMS	4-HBA	50-90 μm	–	–	First microfluidic spinning, enzyme immobilization	34
			50-130 μm	–	–	CFD-based modeling	36
		Alginate	19-55 μm	Encapsulation	L929 (Human fibroblast) cells	Cell and bovine serum albumin (BSA) encapsulation	45
			~20 μm	Encapsulation	L929 cells	–	53
		Alginate/chitosan	100 μm	Adhesion, encapsulation	Human hepatocellular carcinoma (HepG2) cells	–	39
		Chitosan	70-150 μm	Adhesion	HepG2 cells	The potential of bioartificial liver chip	60
		PLGA	20-230 μm	Adhesion	L929 cells, primary rat embryonic cortical neurons	Porous interior with dense outer surface, 3D guided cell growth	56
			10-242 μm	Adhesion	L929 cells (on the surface)	Porous interior with dense outer surface, the effects of fiber diameter on cell orientation	57

		Amphiphilic triblock (PPDO-co-PCL-b-PEG-b-PPDO-co-PCL)	2-200 μm	Encapsulation	L929 cells	Fibronectin release study	69
	Glass chip	Alginate	180-500 μm	Encapsulation	Wharton's Jelly Mesenchymal Stem Cells (WJMSCs)	–	55
	Cyclic Olefin Copolymer (COC)	PEGDMA	100-500 μm	Encapsulation	Bacteria (*E. coli*, *B. cereus*)	Biohybrid fiber with porous surface	82
	PMMA Chip	Alginate	211-364 μm	Encapsulation	Glioblastoma multiforme (GBM) cells	Magnetic-responsive controlled drug release	41
		Chitosan	50-200 μm	Adhesion	Schwann cell, fibroblast cells	Guided cell growth	59
	PDMS	PEGDA	~50 μm	–	–	Controlled length of fiber using valve actuation	29
		Alginate	~100 μm	–	–	Theoretical analysis	93
			7-200 μm	Encapsulation	NIH-3T3 cells, human cervical cancer cells(HeLa), rat pheochromocytoma cells(PC12)	Anisotropic hydrogel fiber for cell guidance	43
			~80 μm	Encapsulation	Primary rat hepatocytes, Swiss 3T3 cells	Scaffold-free hepatic micro-organoids (~50 μm), anisotropic hydrogel fiber	37
		PBI	12-40 μm	–	–	Anhydrous proton conductivity	92
		RSF	20-45 μm	–	–	Silk fiber	73
	PDMS with round channel	Alginate	70-115 μm	–	–	First PDMS-only cylindrical coaxial-flow channels	47
			100-250 μm	–	–	Digital valve control system, tunable physiochemical coding, spindle knot/gas bubble encoded/neutrophil chemoattractant-encoded fibers	48
		Alginate/collagen	250 μm	Encapsulation	Hybrid spheroids of primary rat hepatocytes and rat pancreatic islets	Cell spheroid encapsulation, co-culture, *in vivo* immunoprotection	66
			250 μm	Encapsulation	Primary rat pancreatic islets	*In vivo* immunoprotection	67

Tubular (Hollow)	Home made annular spinneret	PLGA	Outer: 550-710 μm, inner: 260-350 μm	–	–	Porous, permeable, and degradable fiber	58
	Stainless steel tubes (triple-orifice spinneret)	Gtn–HPA	< 1 mm	Encapsulation	Human microvascular endothelial (HME) cells, human proximal tubular (HPT) cells	Cell immobilization	89
		Gtn-HPA with alginate, poly(NIPAAM) or polysulfone	Outer: 300-500 μm, inner: 70-100 μm	Encapsulation	HPT cells	Copolymerization of ECM	70
	PMMA + stainless steel needle, glass capillary, and Teflon capillary	PAN, PSF, or PS	Outer: 300-900 μm, inner: 40-150 μm	–	–	Titanium dioxide (TiO_2) nanoparticle encapsulation	91
	Pulled glass pipettes	Alginate/collagen	< 200 μm	Encapsulation	NIH-3T3 cells, HeLa, MIN6m9, HepG2 cells	Woven cell fabric	63
			Outer: 140 μm, inner: ~60 μm	Encapsulation	NIH-3T3 cells	Woven cell fabric	62
			~500 μm	Encapsulation	MIN6m9	*In vivo* implantation	87
		Alginate with collagen, fibrin, or agarose IPN hydrogel	Outer: 210 μm, inner: 92 μm	Encapsulation	NIH-3T3 cells, C2C12, primary rat cardiomyocytes, primary human endothelial cells, MS1, primary cortical cells, primary mouse neural stem cells, HepG2 cells, MIN6m9, primary rat pancreatic islets, HeLa	Encapsulation of various cells with ECM proteins, reconstruction of functional tissues, fiber assembly by weaving and reeling, *in vivo* implantation	44
	Pulled glass pipettes in PDMS	4-HBA	50-90 μm	–	–	First microfluidic spinning, enzyme immobilization	34
		Alginate	~100 μm	Encapsulation	Calf pulmonary artery endothelial(CPAE) cells	–	54
			Outer: < 250 μm, inner: 0.3 μm	Encapsulation	Endothelial cells (HIVE-78) (in hollow fiber), smooth muscle cells (HIVS-125) (in gel matrix)	Encapsulation of fiber in an agar-gelatin-fibronectin matrix for 3D microvascularized structure	46

			120-250 μm	–	–	Embedding enzyme-entrapped fiber for biocatalytic microchemical reactor	49
		Chitosan, chitosan/gelatin	Outer: 120-185 μm, inner: 70-150 μm	Encapsulation	NIH-3T3 cells	–	61
	PDMS	Two hydrophilic oligomeric phases PEGDA	Outer: 57-77 μm, inner: 24-56 μm	–	–	Complex-shaped microfibers (single hollow, double hollow, and microbelt)	32
Hybrid	PDMS	PU	~50 μm	Adhesion	NIH-3T3 cells	Janus (asymmetric) fiber (porous and nonporous region) using carbon dioxide bubbles	71
	Pulled glass pipettes in PDMS	4-HBA	50-90 μm	–	–	First Microfluidic Spinning	34
	PDMS with round channel	Alginate	100-250 μm	Adhesion, Encapsulation	Primary rat embryonic cortical neurons (on grooved fiber), primary rat hepatocytes and L929 cells (co-culture)	Digital valve control system, tunable physiochemical coding, grooved fiber, spatially controlled co-culture	48
Flat	Teflon chip	4-HBA	Width: 12.2-198 μm, height: 2.6-45 μm	–	–	Groove sheath-flow device for hydrodynamic focusing, fibers with predetermined cross-sectional shape	35
	Teflon chip	PMMA	submicron thickness	–	–		88
	PMMA chip	Mesogen, acrylate	Width: 13-172 μm, height: 10-45 μm	–	–		86
	Polyether ether ketone (PEEK), PDMS chip	Thiol-ene (PETMP, TATATO)	Width: 780 μm, height: 300 μm	–	–	Groove sheath-flow device, double anchor shape (pointed anchor tips < 10 μm)	85
	PDMS	PEGDA	Width: 500 μm	–	–	Mosaicked fiber, multiplex biomolecular analysis	30
	PDMS with flat channel	4-HBA/PEGDA	Width: 240 μm, height: 50 μm	–	–	First flat fiber, enzyme-immobilized barcoded strip for multiple bioanalysis,	33

						programmable actuation to the pH variation	
		Alginate	Height < 10 μm	Adhesion	Primary rat embryonic cortical neurons, rat skeletal muscle cells (L6)	Cell alignment on grooved fiber	50
			Width: 3 mm, height: 150~350 μm	Encapsulation	Primary rat neonatal cardiomyocytes, human umbilical vein endothelial cells (HUVEC)	Mosaic hydrogel sheets, barcoding, cell patterning	52
Scale-down and crystalline structure	Teflon chip	PMMA	> 300 nm	–	–	Groove sheath-flow device for hydrodynamic focusing	88
	Pulled glass tube	Vanadium Pentoxide (V_2O_5)	> 10 nm	–	–	Morphology control of nanofiber assemblies, application for sensing redox-active gases	90
	Pulled glass pipettes	Alginate	50 μm	–	–	Alignment of supramolecular strands	42
	PDMS	Alginate	70 nm-20 μm	–	–	Crystal-like structure by dehydrating IPA sheath flow	51

References

1. R. Langer and J. P. Vacanti, *Science*, 1993, 260, 920-926.
2. U. A. Stock and J. P. Vacanti, *Annual review of medicine*, 2001, 52, 443-451.
3. G. Vunjak-Novakovic and D. T. Scadden, *Cell stem cell*, 2011, 8, 252-261.
4. J. Park, K. Kim, J. Lee, H. Kim and D. Huh, *Biomed. Eng. Lett.*, 2012, 2, 88-94.
5. J. Ng, Y. Shin and S. Chung, *Biomed. Eng. Lett.*, 2012, 2, 72-77.
6. H. Andersson and A. van den Berg, *Lab on a chip*, 2004, 4, 98-103.
7. W. Y. Yeong, C. K. Chua, K. F. Leong and M. Chandrasekaran, *Trends Biotechnol*, 2004, 22, 643-652.
8. A. G. Mikos, A. J. Thorsen, L. A. Czerwonka, Y. Bao, R. Langer, D. N. Winslow and J. P. Vacanti, *Polymer*, 1994, 35, 1068-1077.
9. A. G. Mikos, G. Sarakinos, S. M. Leite, J. P. Vacanti and R. Langer, *Biomaterials*, 1993, 14, 323-330.
10. K. Whang, C. H. Thomas, K. E. Healy and G. Nuber, *Polymer*, 1995, 36, 837-842.
11. K. Whang, D. C. Tsai, E. K. Nam, M. Aitken, S. M. Sprague, P. K. Patel and K. E. Healy, *J Biomed Mater Res*, 1998, 42, 491-499.
12. Y. S. Nam and T. G. Park, *J Biomed Mater Res*, 1999, 47, 8-17.
13. R. Zhang and P. X. Ma, *J Biomed Mater Res*, 1999, 44, 446-455.
14. C. Schugens, V. Maquet, C. Grandfils, R. Jerome and P. Teyssie, *J Biomed Mater Res*, 1996, 30, 449-461.
15. L. D. Harris, B. S. Kim and D. J. Mooney, *J Biomed Mater Res*, 1998, 42, 396-402.
16. S. J. Lee, H. W. Kang, J. K. Park, J. W. Rhie, S. K. Hahn and D. W. Cho, *Biomedical microdevices*, 2008, 10, 233-241.
17. X. Wang, Y. Yan, Y. Pan, Z. Xiong, H. Liu, J. Cheng, F. Liu, F. Lin, R. Wu, R. Zhang and Q. Lu, *Tissue engineering*, 2006, 12, 83-90.
18. R. Landers, U. Hubner, R. Schmelzeisen and R. Mulhaupt, *Biomaterials*, 2002, 23, 4437-4447.
19. S. F. Badylak, *Biomaterials*, 2007, 28, 3587-3593.
20. G. A. Di Lullo, S. M. Sweeney, J. Korkko, L. Ala-Kokko and J. D. San Antonio, *J Biol Chem*, 2002, 277, 4223-4231.
21. H. Yoshimoto, Y. M. Shin, H. Terai and J. P. Vacanti, *Biomaterials*, 2003, 24, 2077-2082.
22. A. R. Tan, J. L. Ifkovits, B. M. Baker, D. M. Brey, R. L. Mauck and J. A. Burdick, *J Biomed Mater Res A*, 2008, 87A, 1034-1043.
23. B. G. Chung, K. H. Lee, A. Khademhosseini and S. H. Lee, *Lab on a chip*, 2012, 12, 45-59.
24. A. Kang, J. Park, J. Ju, G. S. Jeong and S.-H. Lee, *Biomaterials*, DOI: http://dx.doi.org/10.1016/j.biomaterials.2013.12.073.
25. F. M. White, *Viscous Fluid Flow, 2nd edition*, McGraw-Hill, Boston, Second edition edn., 1991.
26. D. J. Beebe, G. A. Mensing and G. M. Walker, *Annual review of biomedical engineering*, 2002, 4, 261-286.
27. F. Zarrin and N. J. Dovichi, *Anal Chem*, 1985, 57, 2690-2692.
28. E. M. V. Kachel, *Flow Cytometry and Sorting, 2nd edtion*, Wiley Press, New York, second edition edn., 1991.
29. J. K. Nunes, K. Sadlej, J. I. Tam and H. A. Stone, *Lab on a chip*, 2012, 12, 2301-2304.
30. S. Cho, T. S. Shim and S. M. Yang, *Lab on a chip*, 2012, 12, 3676-3679.
31. S. C. Laza, M. Polo, A. A. Neves, R. Cingolani, A. Camposeo and D. Pisignano, *Advanced materials*, 2012, 24, 1304-1308.
32. C. H. Choi, H. Yi, S. Hwang, D. A. Weitz and C. S. Lee, *Lab on a chip*, 2011, 11, 1477-1483.
33. S. Kim, H. Oh, J. Baek, H. Kim, W. Kim and S. Lee, *Lab on a chip*, 2005, 5, 1168-1172.
34. W. Jeong, J. Kim, S. Kim, S. Lee, G. Mensing and D. J. Beebe, *Lab on a chip*, 2004, 4, 576-580.
35. A. L. Thangawng, P. B. Howell, Jr., C. M. Spillmann, J. Naciri and F. S. Ligler, *Lab on a chip*, 2011, 11, 1157-1160.
36. J. I. Ju, H. J. Oh, S. R. Kim and S. H. Lee, *J Micromech Microeng*, 2005, 15, 601-607.
37. M. Yamada, R. Utoh, K. Ohashi, K. Tatsumi, M. Yamato, T. Okano and M. Seki, *Biomaterials*, 2012, 33, 8304-8315.
38. S. Sugiura, T. Oda, Y. Aoyagi, M. Satake, N. Ohkohchi and M. Nakajima, *Lab on a chip*, 2008, 8, 1255-1257.
39. B. R. Lee, K. H. Lee, E. Kang, D. S. Kim and S. H. Lee, *Biomicrofluidics*, 2011, 5, 22208.
40. J. Hammer, L. H. Han, X. Tong and F. Yang, *Tissue engineering. Part C, Methods*, 2013, DOI: 10.1089/ten.TEC.2013.0176.
41. Y. S. Lin, K. S. Huang, C. H. Yang, C. Y. Wang, Y. S. Yang, H. C. Hsu, Y. J. Liao and C. W. Tsai, *PloS one*, 2012, 7, e33184.

42. D. Kiriya, M. Ikeda, H. Onoe, M. Takinoue, H. Komatsu, Y. Shimoyama, I. Hamachi and S. Takeuchi, *Angewandte Chemie*, 2012, 51, 1553-1557.
43. M. Yamada, S. Sugaya, Y. Naganuma and M. Seki, *Soft Matter*, 2012, 8, 3122-3130.
44. H. Onoe, T. Okitsu, A. Itou, M. Kato-Negishi, R. Gojo, D. Kiriya, K. Sato, S. Miura, S. Iwanaga, K. Kuribayashi-Shigetomi, Y. T. Matsunaga, Y. Shimoyama and S. Takeuchi, *Nat Mater*, 2013, 12, 584-590.
45. S. Shin, J. Y. Park, J. Y. Lee, H. Park, Y. D. Park, K. B. Lee, C. M. Whang and S. H. Lee, *Langmuir*, 2007, 23, 9104-9108.
46. K. H. Lee, S. J. Shin, Y. Park and S. H. Lee, *Small*, 2009, 5, 1264-1268.
47. E. Kang, S. J. Shin, K. H. Lee and S. H. Lee, *Lab on a chip*, 2010, 10, 1856-1861.
48. E. Kang, G. S. Jeong, Y. Y. Choi, K. H. Lee, A. Khademhosseini and S. H. Lee, *Nat Mater*, 2011, 10, 877-883.
49. A. Asthana, K. H. Lee, S. J. Shin, J. Perumal, L. Butler, S. H. Lee and D. P. Kim, *Biomicrofluidics*, 2011, 5.
50. E. Kang, Y. Y. Choi, S. K. Chae, J. H. Moon, J. Y. Chang and S. H. Lee, *Advanced materials*, 2012, 24, 4271-+.
51. S. K. Chae, E. Kang, A. Khademhosseini and S. H. Lee, *Advanced materials*, 2013, 25, 3071-3078.
52. L. Leng, A. McAllister, B. Zhang, M. Radisic and A. Gunther, *Advanced materials*, 2012, 24, 3650-3658.
53. J. S. Hong, S. J. Shin, S. Lee, E. Wong and J. Cooper-White, *Korea-Aust Rheol J*, 2007, 19, 157-164.
54. S. J. Shin, K. H. Lee and S. H. Lee, San Diego, California, USA, 2008.
55. L. Capretto, S. Mazzitelli, X. Zhang and C. Nastruzzi, Groningen, The Netherlands, 2010.
56. C. M. Hwang, A. Khademhosseini, Y. Park, K. Sun and S. H. Lee, *Langmuir*, 2008, 24, 6845-6851.
57. C. M. Hwang, Y. Park, J. Y. Park, K. Lee, K. Sun, A. Khademhosseini and S. H. Lee, *Biomedical microdevices*, 2009, 11, 739-746.
58. X. Wen and P. A. Tresco, *Biomaterials*, 2006, 27, 3800-3809.
59. C. H. Yeh, P. W. Lin and Y. C. Lin, *Microfluid Nanofluid*, 2010, 8, 115-121.
60. K. H. Lee, S. J. Shin, C. B. Kim, J. K. Kim, Y. W. Cho, B. G. Chung and S. H. Lee, *Lab on a chip*, 2010, 10, 1328-1334.
61. J. Oh, K. Kim, S. W. Won, C. Cha, A. K. Gaharwar, S. Selimovic, H. Bae, K. H. Lee, D. H. Lee, S. H. Lee and A. Khademhosseini, *Biomedical microdevices*, 2013, 15, 465-472.
62. H. Onoe, R. Gojo, Y. Tsuda, D. Kiriya and S. Takeuchi, Wanchai, Hong Kong, 2010.
63. H. Onoe, R. Gojo, Y. Matsunaga, D. Kiriya, M. Kato-Negishi, K. Kuribayashi-Shigetomi, Y. Shimoyama and S. Takeuchi, Cancun, Mexico, 2011.
64. H. Sato, Y. Sasamoto, D. Yagyu, T. Sekiguchi and S. Shoji, *J Micromech Microeng*, 2007, 17, 2211-2216.
65. D. H. Yoon, A. Nakahara, A. Jamshaid, H. Sato, T. Sekiguchi and S. Shoji, *Journal of Sensors*, 2013, 2013, 6.
66. Y. Jun, A. R. Kang, J. S. Lee, G. S. Jeong, J. Ju, D. Y. Lee and S. H. Lee, *Biomaterials*, 2013, 34, 3784-3794.
67. Y. Jun, M. J. Kim, Y. H. Hwang, E. A. Jeon, A. R. Kang, S. H. Lee and D. Y. Lee, *Biomaterials*, 2013, 34, 8122-8130.
68. N. A. Raof, M. R. Padgen, A. R. Gracias, M. Bergkvist and Y. B. Xie, *Biomaterials*, 2011, 32, 4498-4505.
69. M. Marimuthu, S. Kim and J. An, *Soft Matter*, 2010, 6, 2200-2207.
70. M. Hu, R. S. Deng, K. M. Schumacher, M. Kurisawa, H. Y. Ye, K. Purnamawati and J. Y. Ying, *Biomaterials*, 2010, 31, 863-869.
71. J. H. Jung, C. H. Choi, S. Chung, Y. M. Chung and C. S. Lee, *Lab on a chip*, 2009, 9, 2596-2602.
72. S. Rammensee, U. Slotta, T. Scheibel and A. R. Bausch, *P Natl Acad Sci USA*, 2008, 105, 6590-6595.
73. M. E. Kinahan, E. Filippidi, S. Koster, X. Hu, H. M. Evans, T. Pfohl, D. L. Kaplan and J. Wong, *Biomacromolecules*, 2011, 12, 1504-1511.
74. X. Hu, Z. Xu and C. Gao, *Scientific reports*, 2012, 2, 767.
75. Z. Liu, Z. Xu, X. Hu and C. Gao, *Macromolecules*, 2013, 46, 6931-6941.
76. X. B. Huang, X. Y. Zhang, X. G. Wang, C. Wang and B. Tang, *J Biosci Bioeng*, 2012, 114, 1-8.
77. A. Khademhosseini, R. Langer, J. Borenstein and J. P. Vacanti, *P Natl Acad Sci USA*, 2006, 103, 2480-2487.
78. F. Yang, R. Murugan, S. Wang and S. Ramakrishna, *Biomaterials*, 2005, 26, 2603-2610.
79. S. Patel, K. Kurpinski, R. Quigley, H. Gao, B. S. Hsiao, M.-M. Poo and S. Li, *Nano letters*, 2007, 7, 2122-2128.

80. I. Poudel, D. Menter and J. Lim, *Biomed. Eng. Lett.*, 2012, 2, 38-45.
81. D. Y. Park, C. H. Mun, E. Kang, D. Y. No, J. Ju and S. H. Lee, *Biofabrication*, 2013. (in press)
82. M. A. Daniele, S. H. North, J. Naciri, P. B. Howell, S. H. Foulger, F. S. Ligler and A. A. Adams, *Adv Funct Mater*, 2013, 23, 698-704.
83. Y. de Hazan, M. Wozniak, J. Heinecke, G. Muller and T. Graule, *J Am Ceram Soc*, 2010, 93, 2456-2459.
84. T. J. Kang, H. Yoon, J. H. Cheon, H. Jeong, H. Lee and Y. H. Kim, *Compos Sci Technol*, 2011, 71, 1495-1500.
85. D. A. Boyd, A. R. Shields, P. B. Howell and F. S. Ligler, *Lab on a chip*, 2013, 13, 3105-3110.
86. A. R. Shields, C. M. Spillmann, J. Naciri, P. B. Howell, A. L. Thangawng and F. S. Ligler, *Soft Matter*, 2012, 8, 6656-6660.
87. S. Sugimoto, Y. J. Heo, H. Onoe, T. Okitsu, H. Kotera and S. Takeuchi, Seattle, Washington, USA, 2011.
88. A. L. Thangawng, P. B. Howell, J. J. Richards, J. S. Erickson and F. S. Ligler, *Lab on a chip*, 2009, 9, 3126-3130.
89. M. Hu, M. Kurisawa, R. Deng, C. M. Teo, A. Schumacher, Y. X. Thong, L. Wang, K. M. Schumacher and J. Y. Ying, *Biomaterials*, 2009, 30, 3523-3531.
90. D. Kiriya and S. Takeuchi, Paris, France, 2012.
91. W. J. Lan, S. W. Li, Y. C. Lu, J. H. Xu and G. S. Luo, *Lab on a chip*, 2009, 9, 3282-3288.
92. M. M. Hasani-Sadrabadi, J. J. Vandersarl, E. Dashtimoghadam, G. Bahlakeh, F. S. Majedi, N. Mokarram, A. Bertsch, K. I. Jacob and P. Renaud, *Lab on a chip*, 2013, 13, 4549-4553.
93. O. Bonhomme, J. Leng and A. Colin, *Soft Matter*, 2012, 8, 10641-10649.

Figure legends

Figure 1. Overview of the various microfluidic spinning methods used to fabricate fibers, along with the fiber's tissue engineering applications. (Left) Microfluidic platforms, such as pulled glass micropipettes or PDMS-based chips, can be used to prepare a variety of patterned channel shapes. The fibers can be created either by photopolymerizing a sample fluid or through chemical reactions between the sample and sheath fluids undergoing coaxial laminar flow in a microchannel. Depending on the platform and materials, fibers with a variety of shapes and sizes may be produced as biomimetic 3D scaffolds. (Right) For the tissue engineering or organ regeneration applications, specific cells with suitable biochemical and physiochemical factors could be incorporated into engineered fibers and may then be formed into the desired tissue or artificial organ.

Figure 2. Solidification methods for fiber generation. Schematic diagram shows coaxial flow channels in microfluidic platforms and their cross-sections to illustrate the principles underlying the cross-linking process for the generation of microfibers with different materials. Fibers can be produced either by (a) photopolymerization or (b) chemical reactions.

Figure 3. Representative microfluidic platforms to generate fibers (a) A triple-orifice spinneret with five inlets at the top and a single outlet at the bottom. (Reprinted with permission from ref. 70, Copyright 2010 Elsevier.) (b) Double-coaxial microfluidic devices composed of pulled glass capillaries and connectors. (Reprinted with permission from ref. 44, Copyright 2013 Nature Publishing Group.) (c) Pulled glass capillaries integrated in a PDMS platform. (Reprinted with permission from ref. 39, Copyright 2011 AIP Publishing LLC.) (d) A PDMS micro device with rectangular channels, fabricated using standard soft lithography and replica molding techniques. (Reprinted with permission from ref. 43, Copyright 2012 The Royal Society of Chemistry.) (e) PDMS micro device with cylindrical channels using replication of a deflected thin free-standing PDMS membrane. (Reprinted with permission from ref. 67, Copyright 2013 Elsevier. Relevant products are available at www.microFIT.kr.)

Figure 4. Fibers with diverse shapes and dimensions. (a) PLGA microfibers with cylindrical shapes, smooth surfaces, and a porous inner structure. (Reprinted with permission from ref. 56, Copyright 2008 American Chemical Society.) (b) PEG-DA hollow microfibers with different core diameters, depending on the flow rate. (Reprinted with permission from ref. 32, Copyright 2011 The Royal Society of Chemistry.) (c) (Top) Janus microfibers showing two distinctive regions with porous and nonporous regions. (Reprinted with permission from ref. 71, Copyright 2009 The Royal Society of Chemistry.) (Bottom) Spatially controlled microfibers by serial, parallel and mixed coding with various composite solutions. (Reprinted with permission from ref. 48, Copyright 2011 The Royal Society of Chemistry.) (d) (Top) Mosaic hydrogels with desired patterns. (Reprinted with permission from ref. 52, Copyright 2012 John Wiley & Sons, Inc.) (Bottom) Flat alginate fibers prepared with different microgroove patterns on either side. (Reprinted with permission from ref. 50, Copyright 2012 John Wiley & Sons, Inc.) (e) Morphology of multiple nanometer-scale fibers according to the flow rate (alginate-IPA, ml h^{-1}). (Reprinted with permission from ref. 51, Copyright 2013 John Wiley & Sons, Inc.)

Figure 5. Examples of fiber scaffolds for cell encapsulation or guidance toward use in tissue engineering applications. (a) Fiber scaffolds for cell encapsulation. (Left) Primary cardiomyocytes in fibrin fibers undergo spontaneous contraction, and primary HUVECs in collagen fibers form a tubular structure. Both systems preserved the intrinsic cellular morphologies and functions of the cell fibers. (Reprinted with permission from ref. 44, Copyright 2013 Nature Publishing Group.) (Middle) Pancreatic islets were encapsulated in collagen–alginate fibers prior to xenotransplantation to protect the cells from the host immune system. (Reprinted with permission from ref. 67, Copyright 2013 Elsevier.) (Right) Co-culture of hepatocytes and fibroblasts (3T3 cells) in anisotropic alginate microfibers, showing controlled formation of hepatic micro-organoids at day 7 after enzymatic digest of the hydrogel matrix. (Reprinted with permission from ref. [37]67, Copyright 2012 Elsevier.) (b) Fiber scaffold for cell guidance. (Left) Cortical neuron alignment on the flat microgrooved alginate fibers, in comparison to the smooth flat fibers. (Reprinted with permission from ref. 50, Copyright 2012 John Wiley & Sons, Inc.) (Right) L929 fibroblasts grown on PLGA fibers of various diameters displayed distinct cell morphologies. (Reprinted with permission from ref. 57, Copyright 2009 Springer.)

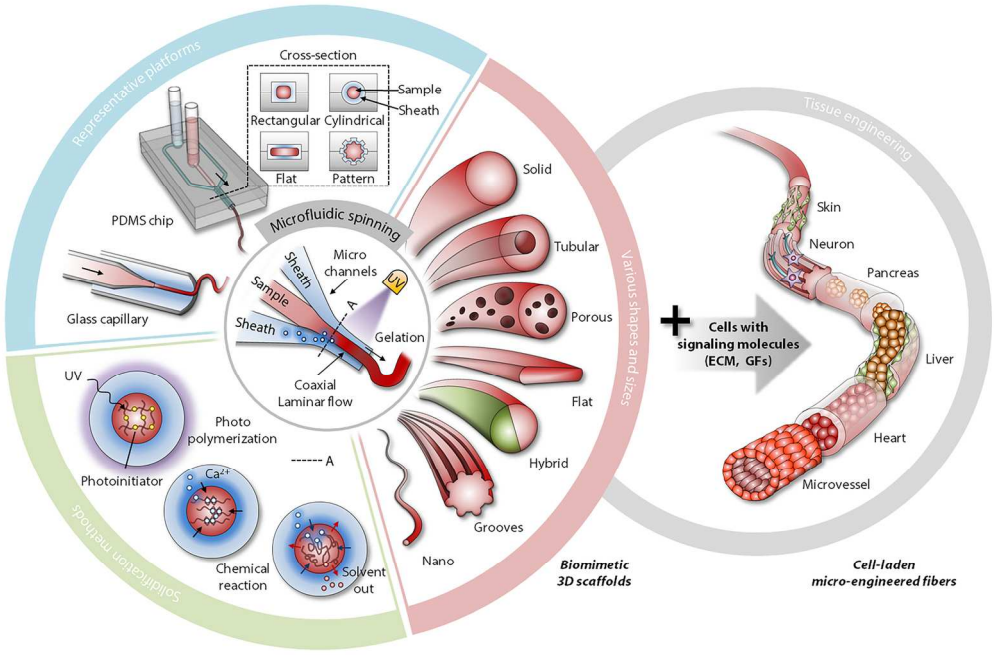

Figure 1. Overview of the various microfluidic spinning methods used to fabricate fibers, along with the fiber's tissue engineering applications. (Left) Microfluidic platforms, such as pulled glass micropipettes or PDMS-based chips, can be used to prepare a variety of patterned channel shapes. The fibers can be created either by photopolymerizing a sample fluid or through chemical reactions between the sample and sheath fluids undergoing coaxial laminar flow in a microchannel. Depending on the platform and materials, fibers with a variety of shapes and sizes may be produced as biomimetic 3D scaffolds. (Right) For the tissue engineering or organ regeneration applications, specific cells with suitable biochemical and physiochemical factors could be incorporated into engineered fibers and may then be formed into the desired tissue or artificial organ.
167x110mm (300 x 300 DPI)

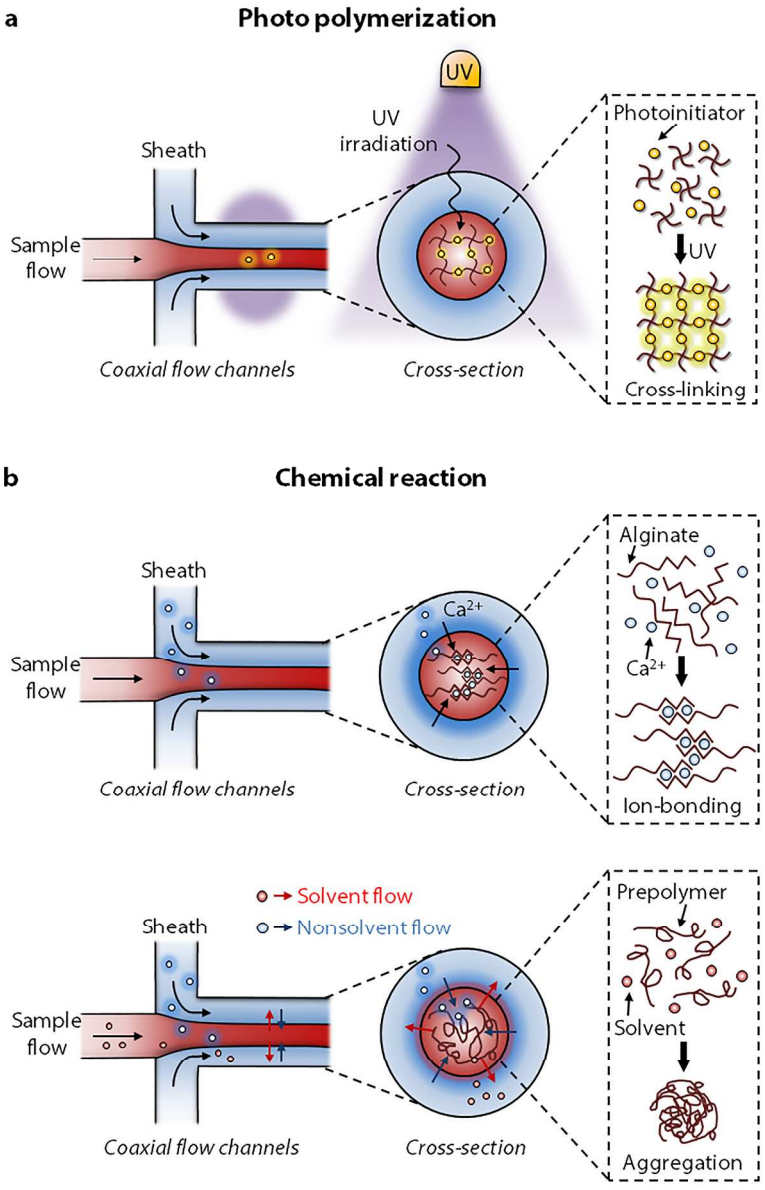

Figure 2. Solidification methods for fiber generation. Schematic diagram shows coaxial flow channels in microfluidic platforms and their cross-sections to illustrate the principles underlying the cross-linking process for the generation of microfibers with different materials. Fibers can be produced either by (a) photopolymerization or (b) chemical reactions.
189x291mm (300 x 300 DPI)

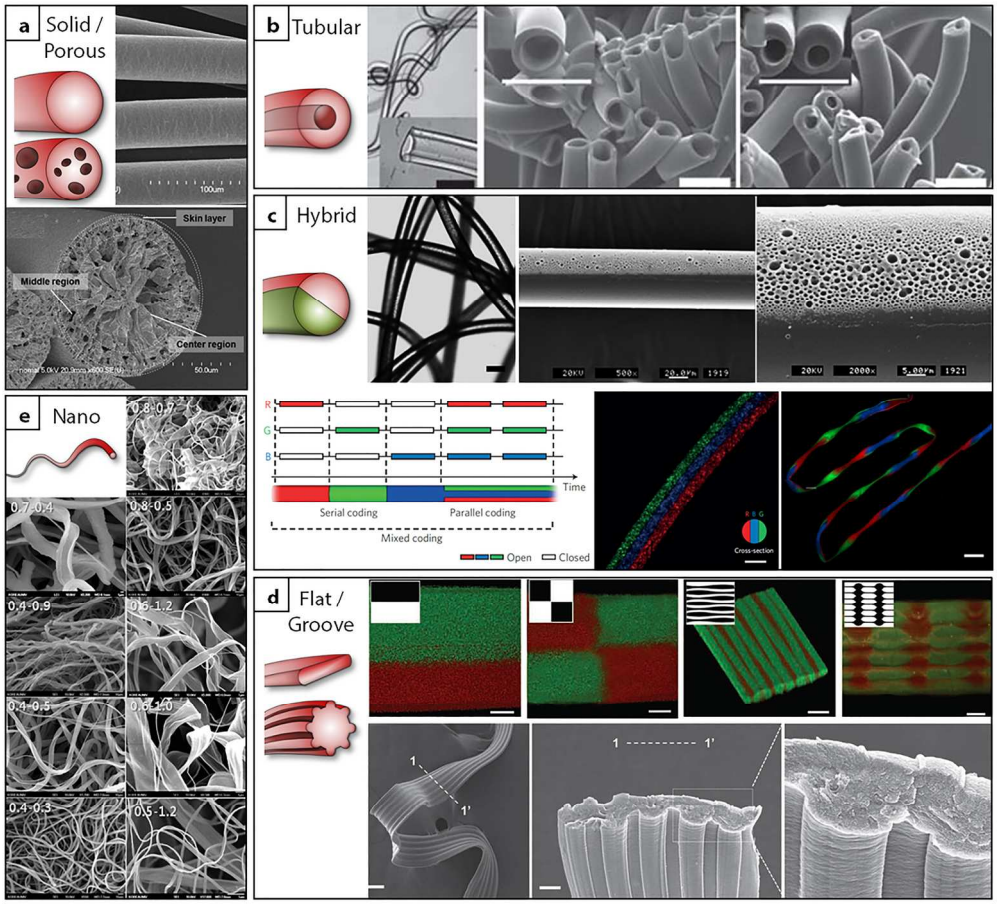

Figure 4. Fibers with diverse shapes and dimensions. (a) PLGA microfibers with cylindrical shapes, smooth surfaces, and a porous inner structure. (Reprinted with permission from ref. 56, Copyright 2008 American Chemical Society.) (b) PEG-DA hollow microfibers with different core diameters, depending on the flow rate. (Reprinted with permission from ref. 32, Copyright 2011 The Royal Society of Chemistry.) (c) (Top) Janus microfibers showing two distinctive regions with porous and nonporous regions. (Reprinted with permission from ref. 71, Copyright 2009 The Royal Society of Chemistry.) (Bottom) Spatially controlled microfibers by serial, parallel and mixed coding with various composite solutions. (Reprinted with permission from ref. 48, Copyright 2011 The Royal Society of Chemistry.) (d) (Top) Mosaic hydrogels with desired patterns. (Reprinted with permission from ref. 52, Copyright 2012 John Wiley & Sons, Inc.) (Bottom) Flat alginate fibers prepared with different microgroove patterns on either side. (Reprinted with permission from ref. 50, Copyright 2012 John Wiley & Sons, Inc.) (e) Morphology of multiple nanometer-scale fibers according to the flow rate (alginate-IPA, ml h-1). (Reprinted with permission from ref. 51, Copyright 2013 John Wiley & Sons, Inc.)
177x161mm (300 x 300 DPI)

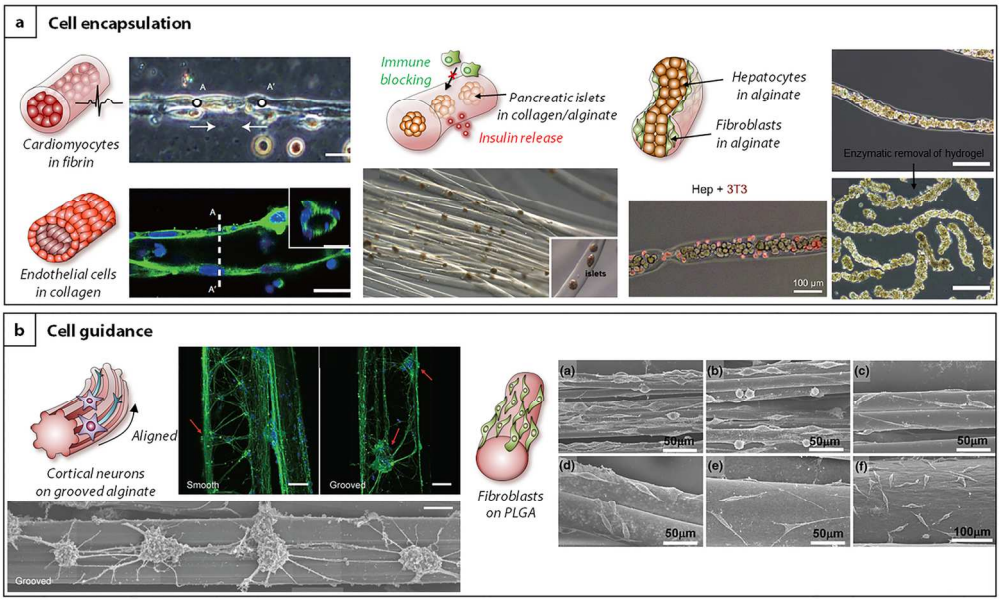

Figure 5. Examples of fiber scaffolds for cell encapsulation or guidance toward use in tissue engineering applications. (a) Fiber scaffolds for cell encapsulation. (Left) Primary cardiomyocytes in fibrin fibers undergo spontaneous contraction, and primary HUVECs in collagen fibers form a tubular structure. Both systems preserved the intrinsic cellular morphologies and functions of the cell fibers. (Reprinted with permission from ref. 44, Copyright 2013 Nature Publishing Group.) (Middle) Pancreatic islets were encapsulated in collagen–alginate fibers prior to xenotransplantation to protect the cells from the host immune system. (Reprinted with permission from ref. 67, Copyright 2013 Elsevier.) (Right) Co-culture of hepatocytes and fibroblasts (3T3 cells) in anisotropic alginate microfibers, showing controlled formation of hepatic micro-organoids at day 7 after enzymatic digest of the hydrogel matrix. (Reprinted with permission from ref. 3767, Copyright 2012 Elsevier.) (b) Fiber scaffold for cell guidance. (Left) Cortical neuron alignment on the flat microgrooved alginate fibers, in comparison to the smooth flat fibers. (Reprinted with permission from ref. 50, Copyright 2012 John Wiley & Sons, Inc.) (Right) L929 fibroblasts grown on PLGA fibers of various diameters displayed distinct cell morphologies. (Reprinted with permission from ref. 57, Copyright 2009 Springer.)
144x86mm (300 x 300 DPI)

Table of contents entry

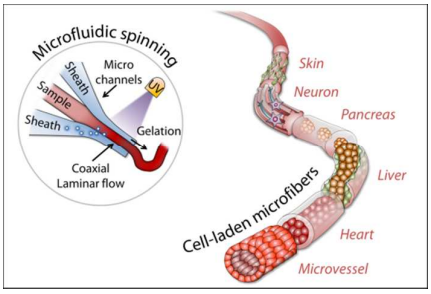

Microfluidic-based spinning techniques for producing micro- and nano-scale fibers, and their potential applications to tissue engineering.